Morphology, Dynamic Mechanical Properties, and Phase Behavior of ABC-Triblock Copolymers with Two Semicompatible Elastomer Blocks

C. Neumann,† D. R. Loveday,‡ V. Abetz,* and R. Stadler

Makromolekulare Chemie II Universität Bayreuth 95440 Bayreuth, Germany

Received October 9, 1997; Revised Manuscript Received January 26, 1998

ABSTRACT: The phase behavior of poly(ethylene-*alt*-propylene)-*block*-poly(ethylene-*co*-butylene)-*block*-polystyrene triblock copolymers with different polystyrene block lengths is investigated by dynamic mechanical analysis, transmission electron microscopy, and small-angle X-ray scattering. While the corresponding poly(ethylene-*alt*-propylene)-*block*-poly(ethylene-*co*-butylene) diblock copolymers show an order−disorder transition in the range of 10−20 °C, the attached polystyrene block prevents the two elastomer blocks from complete mixing in the same temperature range. This is also indicated by the morphologies these triblock copolymers show in comparison to the corresponding nonhydrogenated precursor polymers (poly(1,4-isoprene)-*block*-poly(1,2-butadiene)-*block*-polystyrene).

Introduction

Block copolymers have attracted increasing interest during the past decades.[1−5] The chemical link between different blocks prevents phase separation on a macroscopic length scale, which makes them different from blends of the corresponding homopolymers. While in the phase separation of polymer blends the various transient morphologies are characterized by different length scales, depending on the composition and the phase separation mechanism (spinodal or nucleation and growth), the length scale of the composition fluctuations is fixed by the composition and chain length in block copolymers, both in the homogeneous (disordered) and microphase separated (ordered) state. The finite length scale of the phase separation in block copolymers has implications on the nature of the microphase transition between the ordered and disordered states (for example refs 6−11). More recently also order−order transitions have been studied (for example refs 12 and 13), and cocontinuous morphologies (gyroid, ordered bicontinuous double diamond) have been discussed for these materials besides the classical spherical, cylindrical, and lamellar morphologies.[11,14−19] The gyroid morphology has some similarities with the cocontinuous transient morphologies observed during spinodal decomposition in binary systems[20] but is in contrast to those limited to a rather narrow range of composition. With respect to ternary (or higher) multiblock copolymers, attention mostly was addressed to the formation of new morphologies,[21−24] and this large variety of morphologies has inititiated also theoretical work in order to describe and predict new morphologies for linear ternary triblock copolymers.[25] Cocontinuous morphologies have been found also in ternary triblock copolymers. From the limited data available so far one might conclude a broader composition window. Cocontinuous morphologies seem to be stabilized in systems having a ratio of the segmental interaction parameters between adjacent blocks (χ_{AB}, χ_{BC}) being very different from unity ($\chi_{AB}/\chi_{BC} \gg 1$ or $\chi_{AB}/\chi_{BC} \ll 1$).[21,26] Most of the systems studied so far consist of rather strongly incompatible blocks, and thus no attention was paid to the possibility of microphase transitions in these systems.

A previous paper reported on the phase behavior of poly(1,4-isoprene)-*block*-poly(1,2-butadiene)-*block*-polystyrenes ($I_xB_yS_z^m$) with varying polystyrene block lengths.[27] (The subscripts *x*,*y*,*z* give the weight percentage of the corresponding block, and the superscript *m* is the molar mass in kilograms per mole.) The two elastomer blocks were of approximately equal length in the systems studied in ref 27. The results obtained from dynamic mechanical analysis (DMA) and transmission electron microscopy (TEM) were similar to those of diblock copolymers, indicating that the two elastomer blocks polyisoprene and poly(1,2-butadiene) were mixed with each other over the temperature range under study, while they were demixed from polystyrene at lower temperatures. For systems with not too large polystyrene blocks, mixing with the PS block was observed upon heating.

In this paper, the phase behavior is studied of the hydrogenated analogues of the samples from ref 27, i.e., poly(ethylene-*alt*-propylene)-*block*-poly(ethylene-*co*-butylene)-*block*-polystyrene triblock copolymers ($EP_xEB_yS_z^m$). It is known that poly(ethylene-*alt*-propylene) and poly(ethylene-*co*-butylene) display an upper critical solution temperature, and the corresponding diblock copolymers have been studied in detail by others (see, for example, Rosedale et al.[28] and references cited therein). So far the influence of a third incompatible block on the miscibility of an attached diblock copolymer has rarely been considered by experiment; though theoretical efforts have considered the "tethered chain". In recent theoretical work, strongly incompatible point-like groups at different locations in a diblock copolymer were studied and it was found that depending on the relative solubility parameters of the different components, mixing of the two blocks may be either enhanced or suppressed.[29]

Experimental Section

Materials. The synthesis and characterization of poly(ethylene-*alt*-propylene)-*block*-poly(ethylene-*co*-butylene)-*block*-polystyrene triblock copolymers has been described in detail

† Present address: Stockhausen GmbH, 47705 Krefeld, Germany.

‡ Present address: Baytown Polymers Center, Exxon Chemical Co., 5200 Bayway Dr., Baytown, TX 77520.

S0024-9297(97)01489-7 CCC: $15.00
Published on Web 03/26/1998

Table 1

diblock and triblock copolymer	M_n			microstructure in IB-diblock copolymer (%)					ODT (°C) of diblock copolymer
	PEP	PEB	PS	1,4-I	3,4-I	1,2-B	1,4-B	cycl	
$EP_{53}EB_{47}{}^{45}$	24	21		92	8	90	2	8	$20 > T_{ODT} > 10$
$EP_{50}EB_{44}S_{06}{}^{48}$			3						
$EP_{50}EB_{50}{}^{54}$	27	27		85	15	92		8	$35 > T_{ODT} > 27$
$EP_{45}EB_{45}S_{10}{}^{60}$			6						
$EP_{55}EB_{45}{}^{62}$	34	28		84	16	88	6	6	$20 > T_{ODT} > 17$
$EP_{46}EB_{38}S_{16}{}^{74}$			12						
$EP_{50}EB_{50}{}^{52}$	26	26		90	10	84	8	8	$35 > T_{ODT} > 20$
$EP_{37}EB_{37}S_{26}{}^{70}$			18						

before.[30] In Table 1 the molecular characteristics of the systems are given. The diblock copolymers (poly(ethylene-*alt*-propylene)-*block*-poly(ethylene-*co*-butylene) were obtained by terminating a part of the reaction solution before adding styrene as a third monomer and subsequent hydrogenation.

Physical Characterization. Film specimens were prepared by casting from toluene solutions at room temperature into Petri dishes. The samples were kept under a weak flow of nitrogen for a month and then put under vacuum; after 1 week the temperature was raised to 60 °C and after 3 days raised to 120 °C for 3 h. Then the samples were cooled to room temperature under vacuum. This way of preparation more likely leads to equilibrium morphologies as compared to the preparation from the melt used in a previous study.[30] Dynamic mechanical analysis was performed on a Rheometrics RDAII rheometer equipped with 25 mm parallel plate geometry. For the whole temperature range it was carefully checked that the measurements were performed in the linear viscoelastic region (strain amplitudes between ~2 and ~10%).

The frequency sweeps were carried out in a frequency range from 0.01 up to 500 rad/s. The temperature sweeps were carried out simultaneously at three or four different frequencies. The reason for carrying out the temparature sweeps simultaneously at different frequencies was to avoid different thermal histories in a sequential procedure (one temperature sweep after another at different frequencies). Due to the samples response only a limited frequency range could be used for the temperature sweeps, since one given strain amplitude must yield sufficient torques at a given temperature for all frequencies simultaneously in this experiment. Thus the lowest frequencies in these experiments were larger, and the largest frequencies were smaller than in the frequency sweeps.

Transmission electron micrographs were taken with a Philipps electron microscope operating at 80 kV using ultrathin film specimens obtained by a Reichert-Jung Ultramicrotome. The samples were stained with RuO_4 (which selectively stains the polystyrene domains in these materials) at room temperature. Small-angle X-ray scattering (SAXS) was measured as a function of the scattering vector **s**. ($\mathbf{s} = 2/\lambda \sin\theta$, with 2θ being the scattering angle) with a Kratky Compact Kamera (A. Paar) using Cu Kα radiation ($\lambda = 0.1542$ nm) generated by an Enraf-Nonius generator operated at 36 kV and 16 mA. The data were not desmeared, and no corrections for density fluctuations were carried out. The SAXS served only as a qualitative measure of morphology and an estimate of the domain spacings from the maximum position s^*. SAXS measurements were performed at room temperature unless indicated otherwise.

Results and Discussion

DMA, SAXS, and TEM of EPEBS. In this section we discuss the dynamic mechanical and morphological properties of the different EPEBS with increasing length of the PS block. First the dynamic mechanical behavior of the EPEB-diblock copolymers is discussed. Figure 1a shows isochronic measurements of the storage modulus G' as a function of temperature T for $EP_{53}EB_{47}{}^{45}$. One can clearly observe the transition of the rubber plateau to the terminal flow region at lower frequencies. The corresponding loss tangent curves are shown in Figure 1b. Here the upturn versus higher temperatures also indicates the terminal flow region, while at higher frequencies the maximum at low tem-

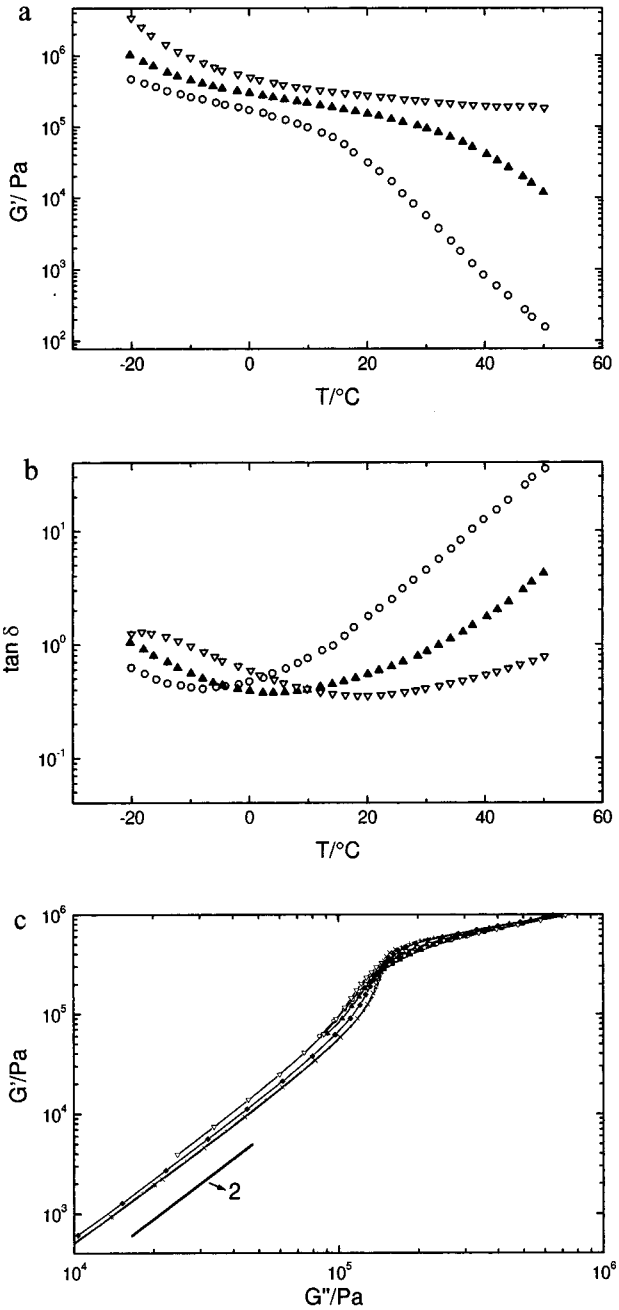

Figure 1. (a) Storage modulus of $EP_{53}EB_{47}{}^{45}$ as a function of temperature for (○) 1, (▲) 10, and (▽) 100 rad/s. (b) Loss tangent of $EP_{53}EB_{47}{}^{45}$ as a function of temperature for (○) 1, (▲) 10, and (▽) 100 rad/s. (c) Han plot of $EP_{53}EB_{47}{}^{45}$ for different temperatures: (■) −20, (○) −10, (▲) −5, (▽) 5, (♦) 10, (+) 20, and (×) 35 °C.

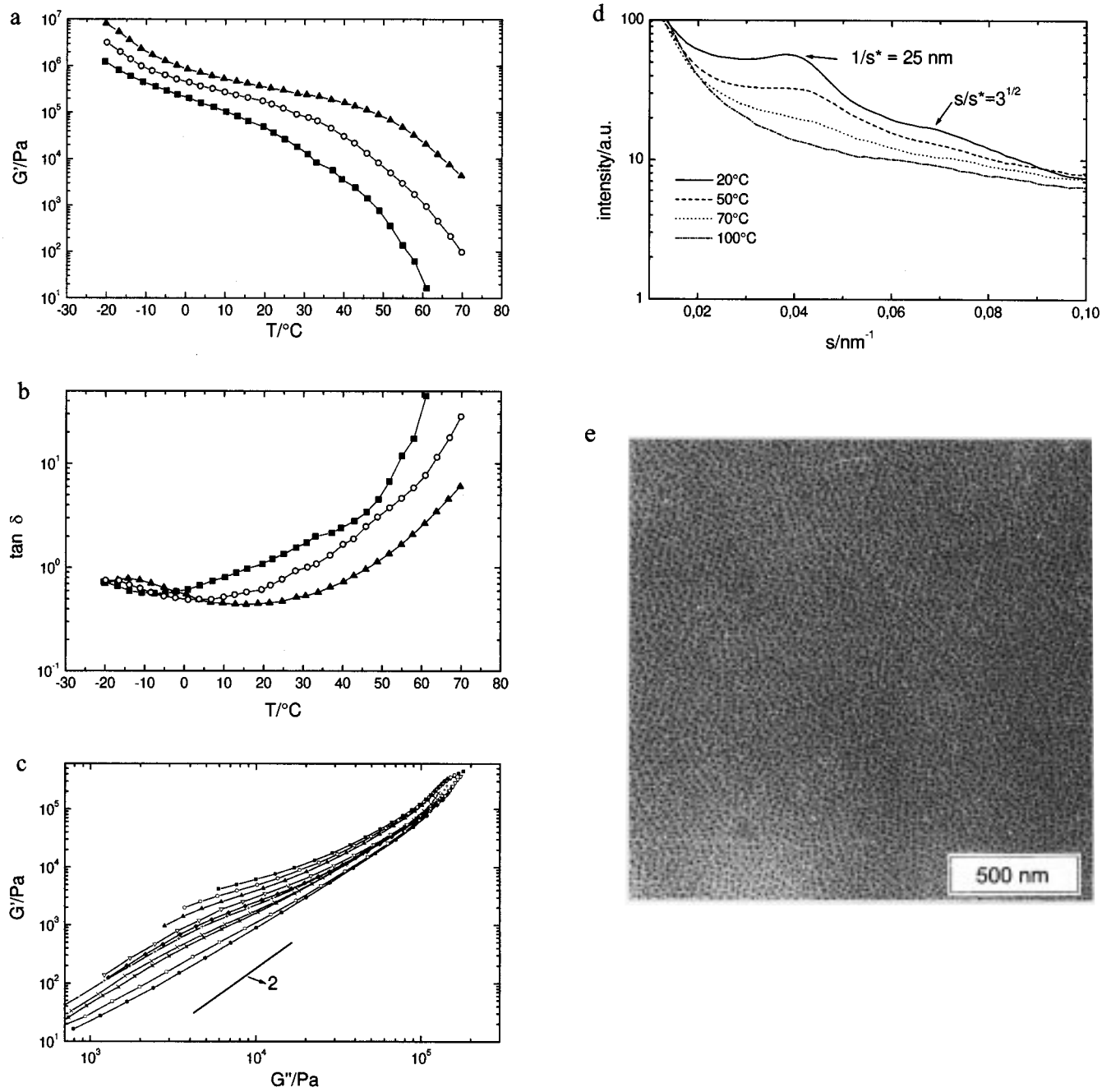

Figure 2. (a) Storage modulus of $EP_{50}EB_{44}S_6^{48}$ as a function of temperature: (■) 0.1, (○) 1, and (▲) 10 rad/s. (b) Loss tangent of $EP_{50}EB_{44}S_6^{48}$ as a function of temperature: (■) 0.1, (○) 1, and (▲) 10 rad/s. (c) Han plot of $EP_{50}EB_{44}S_6^{48}$ for different temperatures: (■) 30, (○) 35, (▲) 40, (▽) 45, (♦) 50, (+) 52, (×) 57, (*) 60, (□) 65, and (●) 70 °C. (d) SAXS traces of $EP_{50}EB_{44}S_6^{48}$ at different temperatures. (e) TEM micrograph of $EP_{50}EB_{44}S_6^{48}$ stained with RuO_4 (polystyrene domains appear dark).

peratures corresponds to the glass transition of the PEB block. The plot G' versus G'' (Han plot) has been shown to be a sensitive way to detect order−disorder transitions (ODT) in diblock copolymers.[31] Although there is a still ongoing discussion about the question of whether or not the first failure of the time−temperature superposition principle can be used as a measure of the ODT,[28] we follow Han's approach here. If all isotherms superimpose, the system is homogeneous; otherwise, the system is microphase separated. As one can see from Figure 1c, the system reaches homogeneity for temperatures above 20 °C, which is indicated by a slope of 2 in this presentation. This slope reflects the typical frequency dependence of G' ($\propto\omega^2$) and G'' ($\propto\omega$) of a homogeneous melt in the terminal flow region. The other diblock copolymers show a similar behavior and therefore are not further discussed here. Their ODT's are listed in Table 1.

The storage modulus G' and the tan δ of the EP_{50}-$EB_{44}S_{06}^{48}$-triblock copolymer are shown as a function of temperature for various frequencies in Figure 2a,b. Here the modulus drops only at higher temperatures from the rubber plateau into the flow region as compared to the corresponding $EP_{53}EB_{47}^{45}$-diblock copolymer shown in Figure 1a. For the lowest frequency, a second inflection point is observed at about 40 °C in Figure 2a, which relates to the glass transition of the short PS block. This corresponds to a maximum in tan δ curve of the same frequency (Figure 2b), which, however, only appears as a shoulder. At higher tem-

peratures, the storage modulus drops rapidly and tan δ increases monotonically, as is typical for a melt. Only for higher frequencies can a maximum at low temperatures be resolved, indicating the glass transition of the PEB block. As one can see from the Han plot (Figure 2c), the slope in the terminal flow region gradually increases toward a value of 2 with increasing temperatures. However, even at the highest measurement temperature a slope of 2 was not reached, which indicates that the system homogenizes at a temperature above 70 °C. To obtain a sufficiently large torque, at 70 °C already a strain amplitude of 23% was necessary for this sample, which became 40% at 80 °C. At smaller amplitudes the torque became too small to be measurable accurately. Since larger strain amplitudes may lead to additional effects such as ordering of the domains,[32] those results are not considered further here. Figure 2d shows the SAXS patterns at different temperatures. The scattered intensity decreases with increasing temperatures and at 70 °C the scattering peak has almost disappeared. This proves a UCST (upper critical solution temperature) type of incompatibility of polystyrene with the two elastomer blocks (since the electron density contrast giving rise to the X-ray scattering exists only between PS on one side and the two elastomer blocks on the other). The scattering peak does not really disappear at high temperatures due to the typical correlations in block copolymers in the disordered state.[6] However, the amount of polystyrene is so small in this polymer that the contribution of the block correlations to the overall scattering becomes very small as compared to the density fluctuations. Besides the reduction in the scattered peak intensity also a slight shift of the peak maximum toward higher **s**-vectors is observed upon increasing temperature, which is a well-known effect of block copolymers in the vicinity of the order−disorder transition.[9,10,33−35] One also observes a broad second peak with a position of $s/s^* = \sqrt{3}$ at the lower temperatures, which disappears upon heating. This second peak could indicate either a spherical (cubic) or a cylindrical (hexagonal) morphology. In Figure 2e the electron micrograph shows spherical PS domains stained by RuO_4 (dark). The distance between the spheres corresponds to the distance obtained from the smeared primary peak in the SAXS pattern ($1/s^* = 25$ nm) at room temperature.

Parts a−c of Figure 3 show the dynamic mechanical behavior of $EP_{45}EB_{45}S_{10}$[60]. The storage modulus (Figure 3a) drops in several pronounced steps. At 0.1 rad/s, above the glass transition of the elastomer blocks the first drop is observed around 20 °C, which is very close to the transition between the rubber plateau and the terminal flow region of the corresponding diblock copolymer. However, the modulus reaches a second plateau here and decreases again around 80 °C (glass transition of the PS block). While, in the diblock copolymer above both the order−disorder transition and the rubber plateau, the chains can relax by reptation, this is impossible for the elastomer blocks fixed to the incompatible PS interface. Here only a relaxation process similar to the retraction modes of the branches in star polymers should be possible, even if the two elastomer blocks are mixed with each other. Above the glass transition temperature the polymer behaves like a structured melt, and only above ca. 160 °C the storage modulus drops significantly again, indicating the onset of melt flow. The corresponding loss tangent curves show a broad maximum related to the inflection point of the storage modulus between the rubber plateau of the two elastomer blocks and the region where PS is still glassy, then a maximum related to the glass transition of PS ($\tan \delta_{max} \approx 80$ °C), and finally a rapid upturn at very high temperatures. The Han plot in Figure 3c again shows the spread due to the glass transition of PS as in Figure 2c. Although the slope increases with increasing temperature, it does not reach the value of 2 within the temperatures investigated in this study. The morphology of this system shows a hexagonal symmetry, as indicated by the relative peak positions in the SAXS pattern at 1, $\sqrt{3}$, $\sqrt{4}$, and $\sqrt{7}$ (Figure 3d), which is maintained up to high temperatures. Thus the order−disorder transition temperature of this system is higher than 250 °C. The long period obtained from SAXS ($1/s^* = 31$ nm at room temperature) compares well with the electron micrograph (Figure 3e), which confirms the formation of the cylindrical PS domains at room temperature.

It is surprising that a system with only 10% PS forms PS cylinders, because in a diblock copolymer a minority component of 10% would form spheres. If we assume the two elastomer blocks to be microphase separated, however, the relative composition of the PS block with respect to its neighboring PEB block is larger (ca. 18%), which makes the occurrence of cylinders more likely. Two possibilities for the morphology may be considered for this polymer. In one case the PEP-end block would form the matrix of a core−shell cylinder consisting of the PS and PEB blocks. In the other case a lamellar morphology of PEP and PEB can be assumed, with PS forming cylinders within the PEB lamellae. To distinguish between these two possibilities, small-angle neutron scattering experiments on samples with one deuterated elastomer block would be very helpful.

The polymer $EP_{46}EB_{38}S_{16}$[74] shows the α-relaxation of PS around 85 °C for the measurement at 0.1 rad/s in Figure 4a,b. This α-relaxation is also observable as a high-temperature shoulder of the large maximum at 1 rad/s and as a low-temperature shoulder of the large maximum at 100 rad/s in Figure 4b. This indicates a stronger dependence of the process associated with the large $\tan \delta_{max}$ as compared with the α-relaxation of PS; i.e., the activation energy of the α-relaxation of PS is much larger. This is even more pronounced in Figure 5b of $EP_{37}EB_{37}S_{26}$[70], where the rather sharp maximum associated with the α-relaxation of PS is appearing at lower temperatures as compared to the broad maximum of the other process and again shows a much weaker frequency dependence. Even at the highest measurement temperatures both systems did not reach the order−disorder transition, as indicated by the slopes less than 2 in the Han plots (Figures 4c, 5c). It seems that the α-relaxation of the PS block influences the shape of the broad peak in tan δ, since that one becomes sharper when occurring above the α-relaxation of PS.

$EP_{46}EB_{38}S_{16}$[74] shows a cylindrical morphology of PS domains at room temperature, which seem not to be hexagonally packed (Figure 4e). The corresponding SAXS pattern shows a rather sharp reflection at $s/s^* = 1.58$, which cannot be assigned to a cubic or hexagonal symmetry. A hexagonal packing of the cylinders can be found at elevated temperatures (160 °C), with $s/s^* = \sqrt{3}$, while cooling again to room temperature restores the original pattern after 1 day. This indicates a thermoreversible effect and could be explained by a

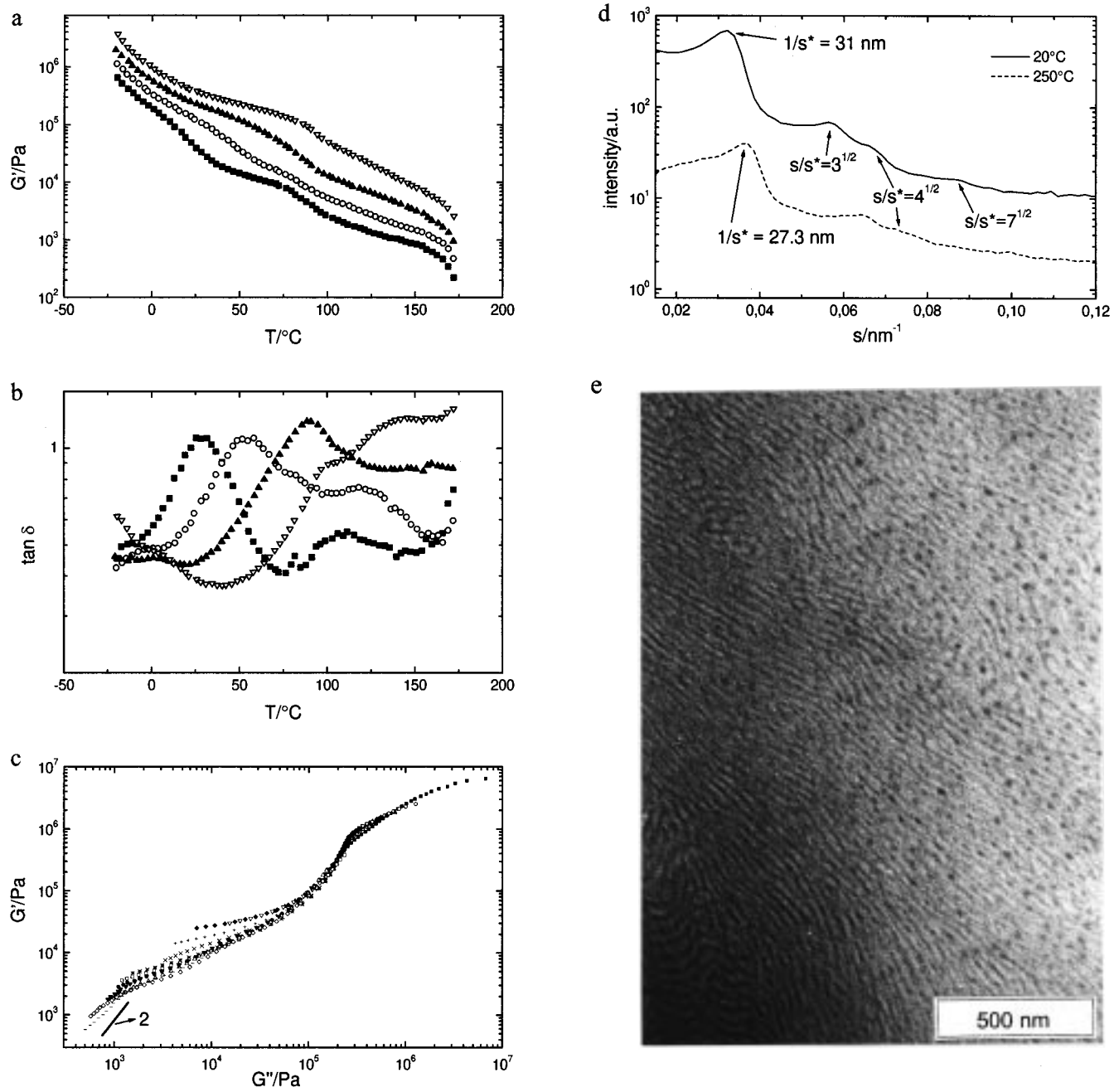

Figure 3. (a) Storage modulus of $EP_{45}EB_{45}S_{10}^{60}$ as a function of temperature: (■) 0.1, (○) 1, (▲) 10, and (▽) 100 rad/s. (b) Loss tangent of $EP_{45}EB_{45}S_{10}^{60}$ as a function of temperature: (■) 0.1, (○) 1, (△) 10, and (▽) 100 rad/s. (c) Han plot of $EP_{45}EB_{45}S_{10}^{60}$ for different temperatures: (■) −10, (○) 10, (▲) 20, (▽) 35, (♦) 50, (+) 65, (×) 80, (*) 90, (□) 100, (●) 110, (△) 120, (▼) 140, (◇) 160, and (—) 180 °C. (d) SAXS traces of $EP_{45}EB_{45}S_{10}^{60}$ at various temperatures. Curves have been displaced vertically for better clarity. (e) TEM micrograph of $EP_{45}EB_{45}S_{10}^{60}$ stained with RuO_4 (polystyrene domains appear dark).

mixing of the two elastomer blocks at high temperatures, leading to a quasi-diblock copolymer with PS cylinders arranged on a hexagonal lattice in a mixed elastomer matrix. At lower temperatures, however, the two elastomer blocks demix from each other and a rhomboedric arrangement of the PS cylinders should be favorable (Figure 4f). From the relative position of the second peak at 1.58 follows an angle of $\alpha = 75.6°$ for the basic plane of the rhomboedric unit cell ($\alpha = 60°$ for a hexagonal unit cell).

The SAXS pattern of $EP_{37}EB_{37}S_{26}^{70}$ shows only rather broad and weak maxima, from which we could not learn much about the morphology. The corresponding electron micrograph at first sight was surprising for us, because it looks like a cocontinuous morphology, although there are only 26% of PS in the system. Following the qualitative argumentation of the occurrence of PS cylinders in $EP_{45}EB_{45}S_{10}^{60}$, we would obtain a relative composition of PS with respect to the neighboring PEB block of ca. 41%, which is within the composition range for gyroid morphologies.[11]

EPEBS in Comparison with IBS. The morphologies and dynamic mechanical behavior of the IBS precursors of the EPEBS triblock copolymers discussed here have been described in detail before.[27] Here we only study the influence of the hydrogenation of the two elastomer blocks. For the IBS-triblock copolymers it was found that they behave like diblock copolymers, due to the miscibility of the two elastomer blocks. Hydrogenation decreases the compatibility of the two elas-

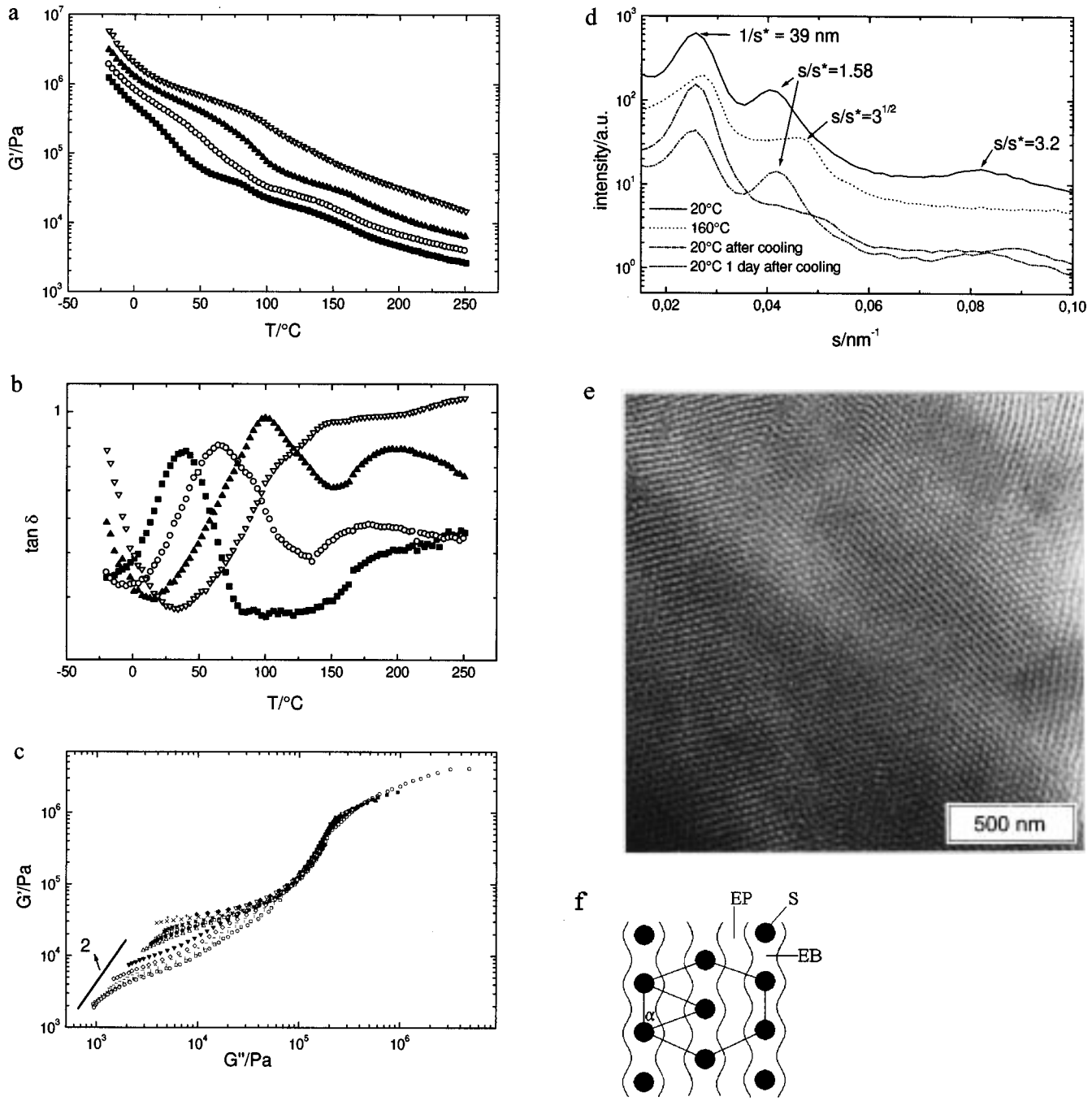

Figure 4. (a) Storage modulus of $EP_{46}EB_{38}S_{16}^{74}$ as a function of temperature: (■) 0.1, (○) 1, (▲) 10, and (▽) 100 rad/s. (b) Loss tangent of $EP_{46}EB_{38}S_{16}^{74}$ as a function of temperature: (■) 0.1, (○) 1, (▲) 10, and (▽) 100 rad/s. (c) Han plot of storage modulus of $EP_{46}EB_{38}S_{16}^{74}$ as a function of frequency: (■) −10, (○) 10, (▲) 20, (▽) 35, (♦) 50, (+) 65, (×) 80, (*) 90, (□) 100, (●) 110, (△) 120, (▼) 140, (◇) 160, (—) 175, (|) 190, (⊡) 210, and (⊙) 230 °C. (d) SAXS traces of $EP_{46}EB_{38}S_{16}^{74}$ at various temperatures. Curves have been displaced vertically for better clarity. (e) TEM micrograph of $EP_{46}EB_{38}S_{16}^{74}$ stained with RuO_4 (polystyrene domains appear dark). (f) Scheme of the basic plane of the rhomboedric unit cell with $\alpha = 75.6°$.

tomer blocks and also increases their incompatibility with polystyrene. This has a great influence on the morphology. In both systems (IBS and EPEBS), electron microscopy only allows discrimination between PS and the elastomer blocks. Thus, we can use a typical morphology scheme of diblock copolymers and compare it with our observations. This is done in Table 2. One observes a shift from the disordered state toward the lamellar morphology upon hydrogenation. The different morphological behavior of the "diblocklike" IBS-triblock copolymers as compared to the EPEBS-triblock copolymers is a strong hint toward microphase separation between the two elastomer blocks in the latter system. This indicates that in fact the PS domains shift the ODT of the attached EPEB-diblock copolymers to higher temperatures. This is probably due to an additional chain stretching of the elastomer blocks, which occurs when they start to mix with each other. The chain stretching is necessary because otherwise the interface with the stronger incompatible PS block would have to increase. Both the increase of stretching and the increase of the interface lead to a larger free energy of the block copolymer chain. Thus, the demixed state remains favorable up to higher temperatures, with respect to the two elastomer blocks, as compared to the corresponding EPEB-diblock copolymers.

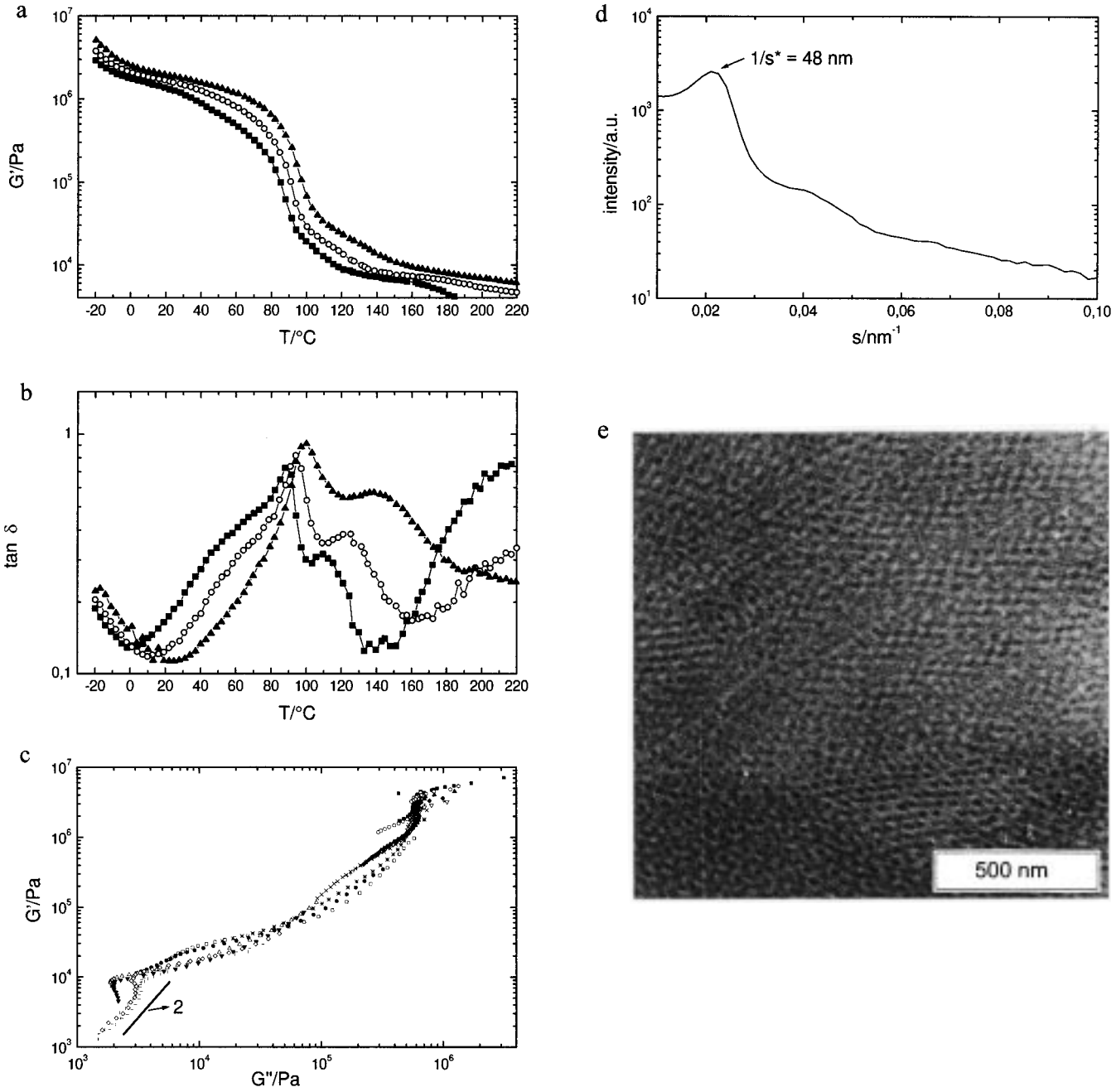

Figure 5. (a) Storage modulus of $EP_{37}EB_{37}S_{26}^{70}$ as a function of temperature: (■) 0.1, (○) 1, and (▲) 10 rad/s. (b) Loss tangent of $EP_{37}EB_{37}S_{26}^{70}$ as a function of temperature: (■) 0.1, (○) 1, and (▲) 10 rad/s. (c) Han plot of storage modulus of $EP_{37}EB_{37}S_{26}^{70}$ as a function of frequency: (■) 20, (○) 40, (▲) 45, (▽) 50, (♦) 60, (+) 70, (×) 80, (*) 90, (□) 100, (●) 110, (△) 130, (▼) 150, (◊) 190, (—) 210, and (|) 230 °C. (d) SAXS trace of $EP_{37}EB_{37}S_{26}^{70}$. (e) TEM micrograph of $EP_{37}EB_{37}S_{26}^{70}$ stained with RuO_4 (polystyrene domains appear dark).

Conclusions

It is important to realize that in comparison to EPEB-diblock copolymers the microphase transition of the two elastomer blocks cannot be determined by the dynamic mechanical behavior alone if a PS block is attached. From DMA only the temperatures of the dynamic glass transitions and the rubber plateaus can be obtained unambiguously in addition to the final disorder transition, i.e., when all three blocks mix. Different techniques are necessary in order to investigate the phase behavior of these ternary systems.

The results show that diblock copolymers connected to a third, incompatible block (or more generally speaking, attached to an internal surface like in a polymer brush) differ in their order−disorder transition behavior from the unperturbed, pure diblock copolymers. Evidence for this behavior was obtained from the comparison of the morphological properties of two different sets

Table 2. Morphological Transitions via Hydrogenation: From IBS to EPEBS

disordered state	spheres	cylinders	cocontinuous morphology	lamellae
$I_{50}B_{44}S_{06}^{48}$	$EP_{50}EB_{44}S_{06}^{48}$			
$I_{45}B_{45}S_{10}^{60}$		$EP_{45}EB_{45}S_{10}^{60}$		
	$I_{46}B_{38}S_{16}^{74}$	$EP_{46}EB_{38}S_{16}^{74}$ [a]		
		$I_{37}B_{37}S_{26}^{70}$	$EP_{37}EB_{37}S_{26}^{70}$	

[a] This polymer shows a rhomboedric arrangement of the cylinders at room temperature.

of triblock copolymers. The influence of hydrogenation on the morphology of triblock copolymers has also been observed for the system polystyrene-*block*-poly(1,2-butadiene)-*block*-poly(methyl methacrylate) (PS−PB−PMMA) in comparison with polystyrene-*block*-poly(ethylene-*co*-butylene)-*block*-poly(methyl methacrylate) (PS−PEB−PMMA), where transitions between a lamellar morphology of PS and PMMA with spheres[22] or cylinders[36] of PB between them and a cylindrical morphology of PS surrounded by PEB rings in a PMMA matrix were found. Also other chemical modifications such as reactions with transition metal complexes may lead to morphological transitions.[37] This gives an additional way to control the morphology of multiblock copolymers by changing the relative incompatibility between the different blocks via polymer analogous reactions.

Acknowledgment. C.N. gratefully acknowledges the help of C. Schleidt during the synthesis of the samples and the assistance of R. Wuerfel during the TEM measurements. V.A. and R.S. thank I. Ya. Erukhimovich (MSU, Moscow), C. C. Han (NIST, Gaithersburg, MD), and L. Leibler (CNRS-Elf Atochem, Paris) for stimulating discussions. Financial support was given by the German Federal Ministry of Education and Science (BMBF) and BASF AG through a joint grant 03M40861 and the German Science Foundation (DFG) through Grant SFB 262, Project S 14.

References and Notes

(1) Molau, G. E. In *Colloidal and Morphological Behaviour of Block Copolymers*; Molau, G. E., Ed.; Plenum Press: New York, 1971.
(2) Riess, G. In *Thermoplastic Elastomers. A Comprehensive Review*; Ledge, N. R., Holden, G., Schroeder, H. E., Eds.; Hanser: Munich, 1987.
(3) Meier, D. J., Ed. *Block Copolymers: Science and Technology*; Gordon & Breach: Tokyo, 1983.
(4) Bates, F. S.; Fredrickson, G. H. *Annu. Rev. Phys. Chem.* **1990**, *41*, 525.
(5) Colby, R. H. *Curr. Opin. Colloid Polym. Sci.* **1996**, *1*, 454.
(6) Leibler, L. *Macromolecules* **1980**, *13*, 1602.
(7) Erukhimovich, I. Ya. *Polym. Sci. USSR* **1982**, *24*, 2223; **1982**, *24*, 2232.
(8) Fredrickson, G. H.; Helfand, E. *J. Chem. Phys.* **1987**, *87*, 697.
(9) Stühn, B. *J. Polym. Sci., Polym. Phys. Ed.* **1992**, *30*, 1013.
(10) Bartels, V. T.; Abetz, V.; Mortensen, K.; Stamm, M. *Europhys. Lett.* **1994**, *27*, 371.
(11) Matsen, M. W.; Bates, F. S. *J. Chem. Phys.* **1997**, *106*, 2436.
(12) Sakurai, S.; Kawada, H.; Hashimoto, T.; Fetters, L. J. *Macromolecules* **1993**, *26*, 5796.
(13) Hajduk, D. A.; Harper, P. E.; Gruner, S. M.; Honeker, C. C.; Kim, G.; Thomas, E. L.; Fetters, L. J. *Macromolecules* **1994**, *27*, 4063.
(14) Matsen, M. W.; Schick, M. *Phys. Rev. Lett.* **1994**, *72*, 2660.
(15) Matsen, M. W.; Bates, F. S. *Macromolecules* **1996**, *29*, 7641.
(16) Erukhimovich, I. Ya. *JETP Lett.* **1996**, *63*, 460.
(17) Hasegawa, H.; Hashimoto, T.; Hyde, S. T. *Polymer* **1996**, *37*, 3825.
(18) Gozdz, W.; Holyst, R. *Macromol. Theory Simul.* **1996**, *5*, 321.
(19) Milner, S. T.; Olmsted, P. T. *J. Phys. II* **1997**, *7*, 249.
(20) Jinnai, H.; Nishikawa, Y.; Koga, T.; Hashimoto, T. *Macromolecules* **1995**, *28*, 4782.
(21) Mogi, Y.; Nomura, M.; Hiroyuli, K.; Ohnishi, K.; Matsushita, Y.; Noda, I. *Macromolecules* **1994**, *27*, 6755.
(22) Stadler, R.; Auschra, C.; Beckmann, J.; Krappe, U.; Voigt-Martin, I.; Leibler, L. *Macromolecules* **1995**, *28*, 3080.
(23) Breiner, U.; Krappe, U.; Stadler, R. *Macromol. Rapid Commun.* **1996**, *17*, 567.
(24) Breiner, U.; Krappe, U.; Abetz, V.; Stadler, R. *Macromol. Chem. Phys.* **1997**, *198*, 1051.
(25) Zheng, W.; Wang, Z.-G. *Macromolecules* **1995**, *28*, 7215.
(26) Jung, K.; Stadler, R.; do Carmo Goncalves, M.; Leibler, L. To be published. Jung, K. Doctoral Dissertation, Johannes Gutenberg-Universität, Mainz, Germany, 1996.
(27) Neumann, C.; Abetz, V.; Stadler, R. *Colloid Polym. Sci.* **1998**, *276*, 19.
(28) Rosedale, J. H.; Bates, F. S.; Almdal, K.; Mortensen, K.; Wignall, G. D. *Macromolecules* **1995**, *28*, 1429.
(29) Erukhimovich, I. Ya.; Abetz, V.; Stadler, R. *Macromolecules* **1997**, *30*, 7435.
(30) Neumann, C.; Abetz, V.; Stadler, R. *Polym. Bull. (Berlin)* **1996**, *36*, 43.
(31) Han, C. D.; Baek, D. M.; Kim, J. K. *Macromolecules* **1990**, *23*, 561.
(32) Wiesner, U. *Macromol. Chem. Phys.* **1997**, *198*, 3319.
(33) Owens, J. N.; Gancarz, I. S.; Koberstein, J. T.; Russell, T. P. *Macromolecules* **1989**, *22*, 3380.
(34) Erukhimovich, I. Ya.; Dobrynin, A. V. *Macromolecules* **1992**, *25*, 4413.
(35) Bartels, V. T.; Stamm, M.; Abetz, V.; Mortensen, K. *Europhys. Lett.* **1995**, *31*, 81.
(36) Breiner, U. Doctoral Dissertation, Johannes Gutenberg-Universität, Mainz, Germany, 1996.
(37) Bronshtein, L.; Seregina, M.; Valetsky, P.; Breiner, U.; Abetz, V.; Stadler, R. *Polym. Bull. (Berlin)* **1997**, *39*, 361.

MA971489S